University of Nebraska - Lincoln

DigitalCommons@University of Nebraska - Lincoln

U.S. Environmental Protection Agency Papers

U.S. Environmental Protection Agency

2017

ATP Binding Cassette Sub-family Member 2 (ABCG2) and Xenobiotic Exposure During Early Mouse Embryonic Stem Cell Differentiation

Mitchell B. Rosen

Susan C. Jeffay

Harriette P. Nichols

Maria R. Hoopes

E. Sidney Hunter III
U.S. Environmental Protection Agency, hunter.sid@epa.gov

Follow this and additional works at: https://digitalcommons.unl.edu/usepapapers

Part of the Earth Sciences Commons, Environmental Health and Protection Commons, Environmental Monitoring Commons, and the Other Environmental Sciences Commons

Research Article
ATP Binding Cassette Sub-family Member 2 (ABCG2) and Xenobiotic Exposure During Early Mouse Embryonic Stem Cell Differentiation

Mitchell B. Rosen 🄳, Susan C. Jeffay, Harriette P. Nichols, Maria R. Hoopes, and E. Sidney Hunter III*

Background: ATP binding cassette sub-family member 2 (ABCG2) is a well-defined efflux transporter found in a variety of tissues. The role of ABCG2 during early embryonic development, however, is not established. Previous work which compared data from the ToxCast screening program with that from in-house studies suggested an association exists between exposure to xenobiotics that regulate Abcg2 transcription and differentiation of mouse embryonic stem cells (mESC), a relationship potentially related to redox homeostasis. **Methods:** mESC were grown for up to 9 days. Pharmacological inhibitors were used to assess transporter function with and without xenobiotic exposure. Proliferation and differentiation were evaluated using RedDot1 and quantiative reverse transcriptase-polymerase chain reaction, respectively. ABCG2 activity was assessed using a Pheophorbide a-based fluorescent assay. Protein expression was measured by capillary-based immunoassay. **Results:** ABCG2 activity increased in differentiating mESC. Treatment with K0143, an inhibitor of ABCG2, had no effect on proliferation or differentiation. As expected, mitoxantrone and topotecan, two chemotherapeutics, displayed increased toxicity in the presence of K0143. Exposure to K0143 in combination with chemicals predicted by ToxCast to regulate ABCG2 expression did not alter xenobiotic-induced toxicity. Moreover, inhibition of ABCG2 did not shift the toxicity of either tert-Butyl hydroperoxide or paraquat, two oxidative stressors. **Conclusion:** As previously reported, ABCG2 serves a protective role in mESC. The role of ABCG2 in regulating redox status, however, was unclear. The hypothesis that ABCG2 plays a fundamental role during mESC differentiation or that regulation of the receptor by xenobiotics may be associated with altered mESC differentiation could not be supported.

Introduction

ATP binding cassette sub-family member 2 (ABCG2), also known as breast cancer resistance protein (BCRP1), is a member of the highly conserved ABC transporter super-family. ABCG2 is a commonly studied multidrug resistance efflux transporter that, along with ABCB1 (P-glycoprotein or Mdr1) and ABCC1(Mrp1), is capable of imparting properties of chemotherapeutic drug resistance and xenobiotic protection. ABCG2 is found in the plasma membrane as a half-transporter with the ability to form functional homodimers or possibly higher-order multimers in a variety of tissues such as small intestine, liver, placenta, mammary gland, brain, kidney, and testis. There is substantial functional overlap among the three ABC multidrug resistance transporters as well as significant structural diversity among those compounds known to be substrates for these transporters (for reviews see Sarkadi et al., 2004; Adachi et al., 2007; Hardwick et al., 2007; Sharom, 2008; Robey et al., 2009; Mo and Zhang, 2012; Stacy et al., 2013).

In addition to its role as a xenobiotic transporter, ABCG2 is highly expressed in certain stem cell populations where it may play a role in maintaining cells in an uncommitted state. ABCG2 activity, for example, is associated with the side-population or "SP" phenotype which was first characterized as a population of uncommitted hematopoietic stem cells with increased capacity for efflux of Hoechst 33342 (Goodell et al., 1996). Although initially associated with ABCB1, ABCG2 has subsequently been shown to be a significant contributor to the SP phenotype (Zhou et al., 2001; Scharenberg et al., 2002). SP cells have been demonstrated in a variety of adult and developing tissues (Kim and Morshead, 2003; Martin et al., 2004; Cervello et al., 2010; Oka et al., 2010; Fatima et al., 2012; Foster et al., 2013). Hence, both ABCB1 and ABCG2 have been evaluated as potential markers of plasticity in various

stem cell populations (for reviews see Bunting, 2002; Ding et al., 2010).

Although ABCG2 is expressed in stem cell populations, the role of the transporter in these cells is not fully understood. SP cells have been identified within the larger population of mouse embryonic stem cells (mESC) as a group of pluripotent but somewhat heterogeneous cells which display characteristics of the inner cell mass and early epiblast (Vieyra et al., 2009). RNA-interference mediated inhibition of ABCG2 or functional blockage of the transporter with fumitremorgin C (FTC) has been shown in mESC to induce cell cycle arrest and reduce expression of Nanog, a key regulator of stem cell pluripotency, thus, raising the possibility that ABCG2 may play a role in stem cell maintenance and colony expansion (Susanto et al., 2008). Conversely, Zhou et al. (2001) found equivalent expression of Abcg in SP and non-SP populations of mESC and Erdei et al. (2013) reported that the expression of pluripotency markers in human embryonic stem cells was independent of ABCG2 expression. Furthermore, *Abcg2*-null mice display a normal phenotype unless faced with a xenobiotic challenge such as pheophorbide a-induced phototoxicity (Jonker et al., 2002).

A previous evaluation by our group of 310 ToxCast Phase 1 chemicals (www.epa.gov/chemical-research/toxcast-dashboard) suggested an association exists between compounds that modify ABCG2 expression and altered differentiation of mESC. In this study, altered redox homeostasis was offered as a potential mode of action for ABCG2 and other pathways proposed to modify mESC differentiation (Chandler et al., 2011). Indeed, regulation of *ABCG2* is complex and its promoter contains multiple *cis*-regulatory elements including response elements for hypoxia and oxidative stress (reviewed by Nakanishi and Ross, 2012). Krishnamurthy et al. (2004) reported that ABCG2 provides resistance to hypoxia in hematopoietic cells and Susanto et al. (2008) suggested that ABCG2 serves to protect embryonic stem cells from oxidative stress by eliminating protoporphyrin IX under conditions of rapid colony expansion. These findings support a role for ABCG2 in maintaining redox homeostasis in embryonic stem cells during conditions of clonal expansion or xenobiotic stress.

This study tested the hypothesis that a causal link exists between altered ABCG2 activity and chemical-induced effects on early mESC differentiaion. Xenobiotic challenge, including exposure to certain ToxCast Phase I compounds and oxidative stress, was used either with or without pharmacological inhibition of ABCG2. mESC were evaluated for changes in cell proliferation and marker gene expression.

Materials and Methods

CHEMICALS

All chemicals were purchased from Sigma-Aldrich (St. Louis, MO) unless otherwise indicated. With the exception of paraquat, all stock solutions were prepared in 100% dimethyl sulfoxide and stored as aliquots at -80°C. Paraquat was prepared as a stock solution in sterile phosphate buffered saline (PBS) and stored as aliquots at -80°C. ToxCast chemicals chosen for evaluation included Propiconazole (CAS 60207-90-1), Flusilazole (CAS 85509-19-9), Pyridaben (CAS 96489-71-3), Rotenone (CAS 83-79-4), and Imazapyr (CAS 81334-34-1).

CELLS

Pluripotent J1 mESC were purchased from ATCC (D3: CRL-1934[TM], J1: SCRC-1010[TM], Manassas, VA) and maintained following protocols adapted from ATCC. Culture methods were described previously (Barrier et al., 2011). In brief, pluripotent mESC were grown in gelatin-coated T25 vented tissue culture flasks (Corning #30639, Corning Life Sciences, Tewsbury, MA) at 37°C in a humidified incubator containing 5% CO_2. Maintenance media contained Knockout Dulbecco's modified eagle's medium (ThermoFisher/Gibco, Grand Island, NY), 15% fetal bovine serum (FBS, ThermoFisher/Gibco), 2 mM GlutaMAX (ThermoFisher/Gibco), 0.1 mM nonessential amino acids (ThermoFisher/Gibco), 50 U/ml Pen/Strep (ThermoFisher/Gibco), and 10 μg/ml Leukemia Inhibiting Factor (EMD Millipore, Billerica, MA). Maintenance cultures of undifferentiated mESC included a feeder layer of mitomycin-c-inactivated mouse embryo fibroblasts (PMEF-CF, EMD Millipore). Cells were passaged every 2 to 3 days at 70 to 80% confluence following digestion with TrypLE Express (ThermoFisher/Gibco) using an initial density of 1×10^6 cells/flask. Cell density was determined using a NucleoCounter[TM] Automatic Cell Counter (New Brunswick Scientific, Edison, NJ). Mouse embryonic fibroblasts were maintained in Dulbecco's modified eagle's medium containing 10% FBS, 2 mM GlutaMAX, and 50 U/ml Pen/Strep.

PLATING AND TREATMENT OF MESC

Before treatment, mouse embryonic fibroblasts were removed using MACS® Technology as directed by the manufacturer (Miltenyi Biotec, San Diego, CA). Enriched pluripotent mESC were then seeded onto 0.1% gelatin-coated 96-well plates in 100 μl media without Leukemia Inhibiting Factor at a density of 2500 cells/well and allowed to attach for 24 hr. A total of 150 μl control or treatment media was then added to each well of the culture plate on the morning of culture day 1. The dimethyl sulfoxide concentration was maintained at 0.1% in all control and treatment wells. Cells were grown at 37°C in a humidified incubator containing 5% CO2 and cultures were terminated on day 4, a useful early culture time point with clearly defined changes in gene expression that were generally analogous to gastrulation in the whole embryo. In those experiments designed to evaluate the role of ABCG2 in mESC following exposure to ToxCast chemicals, control and treatment media were refreshed on a daily basis beginning on day 4 and cultures terminated on day 9, a

TABLE 1. *Genes Used for Reverse Transcriptase-Polymerase Chain Reaction in mESC.*

Gene name	Gene symbol	Marker type	Taqman assay
Actin, beta	*Actb*	Housekeeping	Mm00607939_s1
Nanog	*Nanog*	Pluripotency	Mm02384862_g1
POU class 5 homeobox1	*Pou5f1*	Pluripotency	Mm00658129_gH
Brachyury	*T*	Gastrulation/Mesendoderm	Mm00436877_m1
Goosecoid	*Gsc*	Gastrulation/Mesendoderm	Mm00650681_g1
Bone morphogenetic protein 4	*Bmp4*	Mesendoderm/Mesoderm	Mm00432087_m1
GATA binding protein 4	*Gata4*	Mesendoderm/Endoderm	Mm00484689_m1
Transthyretin	*Ttr*	Mesendoderm/Endoderm	Mm00443267_m1
Neural cell adhesion molecule 1	*Ncam1*	Ectoderm	Mm01149710_m1
Nestin	*Nes*	Ectoderm	Mm00450205_m1
Desmin	*Des*	Mesoderm	Mm00802455_m1
Myosin, heavy polypeptide 7	*Myh7*	Cardiomyocyte	Mm01319006_g1
Myosin, light polypeptide 4	*Myl4*	Cardiomyocyte	Mm00440378_m1
ATP-binding cassette,sub-familyG, mem2	*Abcg2*		Mm0049634_m1
ATP-binding cassette, sub-familyB, mem1	*Abcb1*		Mm00440736_m1
ATP-binding cassette, sub-familyC, mem1	*Abcc1*		Mm00456156_m1

time point associated with a robust cardiomyocyte gene signature. This was done to evaluate cells at a similar time point to that used in previous studies (Barrier et al., 2011; Chandler et al., 2011).

EVALUATION OF MESC PROLIFERATION AND TRANSPORTER ACTIVITY

Cell number was estimated directly in culture plates by washing 1× with PBS followed by fixing for 20 min in 4% neutral buffered formalin. The cells were then washed 4× in PBS plus 0.1% Triton X100, 5 min each, and stained with 1:1000 RedDot1 (Biotium Inc., Fremont, CA) in PBS for 30 min. After staining, cells were washed 4× in PBS plus 0.1% tween 20 for 5 min each and allowed to air dry for a minimum of 48 hr before fluorescence determination using the 700 nm channel of a LI-COR Odyssey near IR plate scanner (Li-Cor Biosciences, Lincoln, NE).

K0143, a chemical inhibitor of ABCG2 (Allen et al., 2002), and pheophrobide a (PhA), a specific fluorescent substrate of ABCG2 and a compound used to measure ABCG2 activity (Henrich et al., 2006), were initially evaluated for utility in our adherent culture system. K0143 was evaluated alongside its more commonly used congener, FTC. Verapamil and MK571, pharmacological inhibitors of ABCB1 and ABCC1, respectively, were assessed as well. mESC were treated on culture day 1 with transporter inhibitors at a concentration range of 0 to 20 μM. 1 μM PhA was added on culture day 3, approximately 20 hr before plate scanning. The culture plate wells were then washed 3× in PBS and scanned on a Spectramax M5 plate scanner (Molecular Devices, Sunnyvale, CA) at excitation and emission wavelengths of 395 and 670 nm, respectively. After scanning, mESC were stained with RedDot1 to normalize fluorescent signal to cell number. K0143 was used at a concentration of 1 μM for all subsequent experiments.

Modifications to the above protocols were used to evaluate ABCG2 activity in early culture where cell number was limited and loss of cells after plate washing was observed. Therefore, to achieve adequate signal, culture plates to be evaluated on day 1 were initially seeded at a density of 30,000 rather than 2500 cells per well using 250 μl media containing K0143 and PhA at a concentration of 1 μM each. The plates were then fixed in neutral buffered formalin for 5 min before washing with PBS and scanning. Day 4 culture plates used for comparison to those scanned on culture day 1 were concurrently seeded with 2500 cells per well in 250 μl media, treated with 1 μM K0143 and PhA on culture day 3, and similarly fixed and scanned on culture day 4.

CAPILLARY-BASED IMMUNOASSAY

mESC were harvested on culture days 0, 2, 4, 6, and 9. Collected cells were lysed in RIPA buffer (ProteinSimple, San Jose, CA) containing inhibitors for both phosphatase and protease (EMD Millipore) at 100 ng each. Lysates were stored at −20°C. Protein concentration was determined using a Bradford Protein Assay kit according to manufacturer's directions (BioRad, Hercules, CA) with absorbance measured on a CLARIOstar microplate reader (BMG Labtech, Cary, NC) at 595 nm.

Protein expression analysis was conducted as directed by the manufacturer on a Wes automated capillary-based immunoassay platform (ProteinSimple, San Jose, CA) using antibodies to ABCG2 (#GTX12131, GeneTex, Irvine, CA) and GAPDH (#NB300-325, Novus Biologicals, Littleton, CO). Chemiluminesce peak area was calculated by Gaussian fit using Compass Software (version 3.1.7) and normalized to GAPDH. One hundred nanograms of sample was used per assay with antibody dilutions for ABCG2 and GAPDH set at 1:300 and 1:200, respectively.

RNA PREPARATION AND CDNA SYNTHESIS

Total RNA was extracted using either TRIzol reagent (ThermoFisher/Invitrogen) or RNAzol (Sigma-Aldrich) according to vendor protocols by removing culture media and adding lysis buffer directly to the wells of culture plates. In general, four identically treated wells were pooled per culture plate to ensure adequate RNA yield. Recovered RNA was resuspended in RNase free water and quantified using a ND-1000 NanoDrop spectrophotometer (ThermoFisher). One microgram preparations were then treated with RNase-free DNase (Promega) and cDNA synthesized using a high capacity cDNA reverse transcription kit (ThermoFisher/Applied Biosystems) according to vendor-supplied protocols. cDNA was diluted to approximately 5 ng/μl assuming 100% reaction efficiency before conducting Taqman assays.

TAQMAN REAL-TIME REVERSE TRANSCRIPTASE-POLYMERASE CHAIN REACTION

Transcripts used for analysis are provided in Table 1. Genes were selected based upon either common usage or on unpublished data from our group which showed a robust response across culture days. Amplifications were conducted in 384 well plates using 12-μl reaction volumes and amplification conditions provided by the vendor (ThermoFisher/Applied Biosystems). All samples were run on an ABI model 7900HT sequence detection system according to the protocol supplied by the manufacturer. Results were summarized using the $2^{-\Delta\Delta Ct}$ method (Livak and Schmittgen, 2001).

STATISTICAL ANALYSIS

A biological replicate was considered the basic unit of analysis and was defined as an individual culture plate grown from a unique seeding of mESC. Replicate wells within a culture plate were considered technical replicates and averaged before statistical analysis. All data were based on three independent biological replicates unless otherwise indicated. Data were analyzed within JMP version 7.0 (SAS, Cary, NC) by analysis of variance. Where possible, experiment was included along with treatment as model main effects. A Tukey-Kramer Honest Significant Difference test was used for posthoc testing with a value of $p \leq 0.05$ used to determine significance.

Results

DIFFERENTIATION OF MESC GROWN IN TWO-DIMENSIONAL ADHERENT CULTURE

Marker gene expression in untreated J1 cells is shown across culture days in Figure 1A. Expression of Nanog and Pou5f1, two standard markers of pluripotency (Nichols et al., 1998; Mitsui et al., 2003), decreased over the culture period, whereas, T (Brachyury) and Gsc, prospective markers of vertebrate gastrulation (De Robertis et al., 1994), peaked around culture day 4. There is a distinct preference for formation of mesodermally-derived cardiomyocytes when mESC are grown under maintenance conditions in media containing serum, hence, genes associated with cardiomyocyte differentiation such as *Bmp4*, *Des*, *Myl4*, and *Myh7* (Winnier et al., 1995; Hofner et al., 2007; Christoforou et al., 2008; Kattman et al., 2011; Bag et al.,
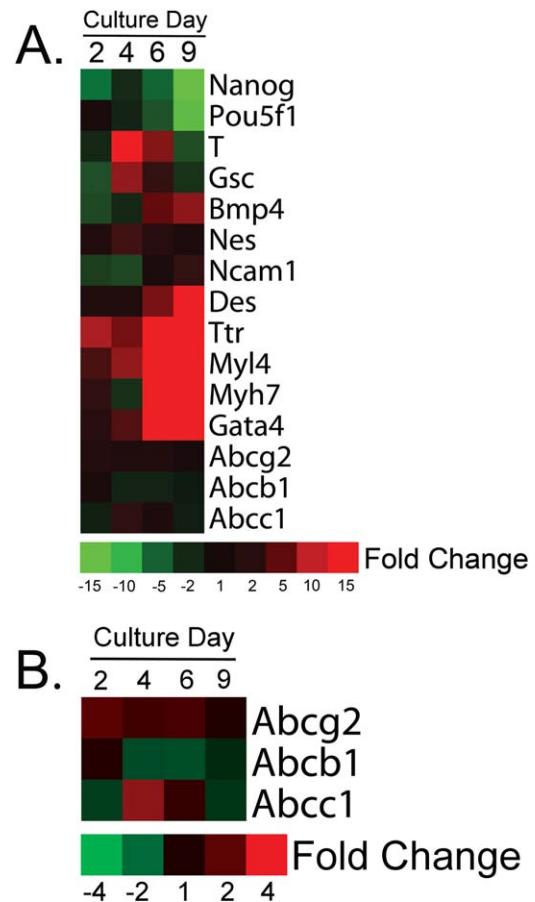
FIGURE 1. *Marker gene expression in untreated mESC. mESC grown in nondirected 2D cultures are predisposed to differentiate into cardiomyocytes, hence, increased expression of genes such as* Bmp4, Des, Myl4, *and* Myh7 *were observed (**A**). Relative to other transcripts, expression of genes coding for ABC efflux transporters remained relatively constant across the culture period (**B**). Data are relative to culture day 0 and represent a single biological replicate from pooled samples.*

FIGURE 2. *Pharmacological inhibition of ABCG2 in mESC. Maximum inhibition of ABCG2 was observed at approximately 1 μM FTC or K0143 based on retention of PhA, a specific fluorescent substrate of ABCG2. Minimal ef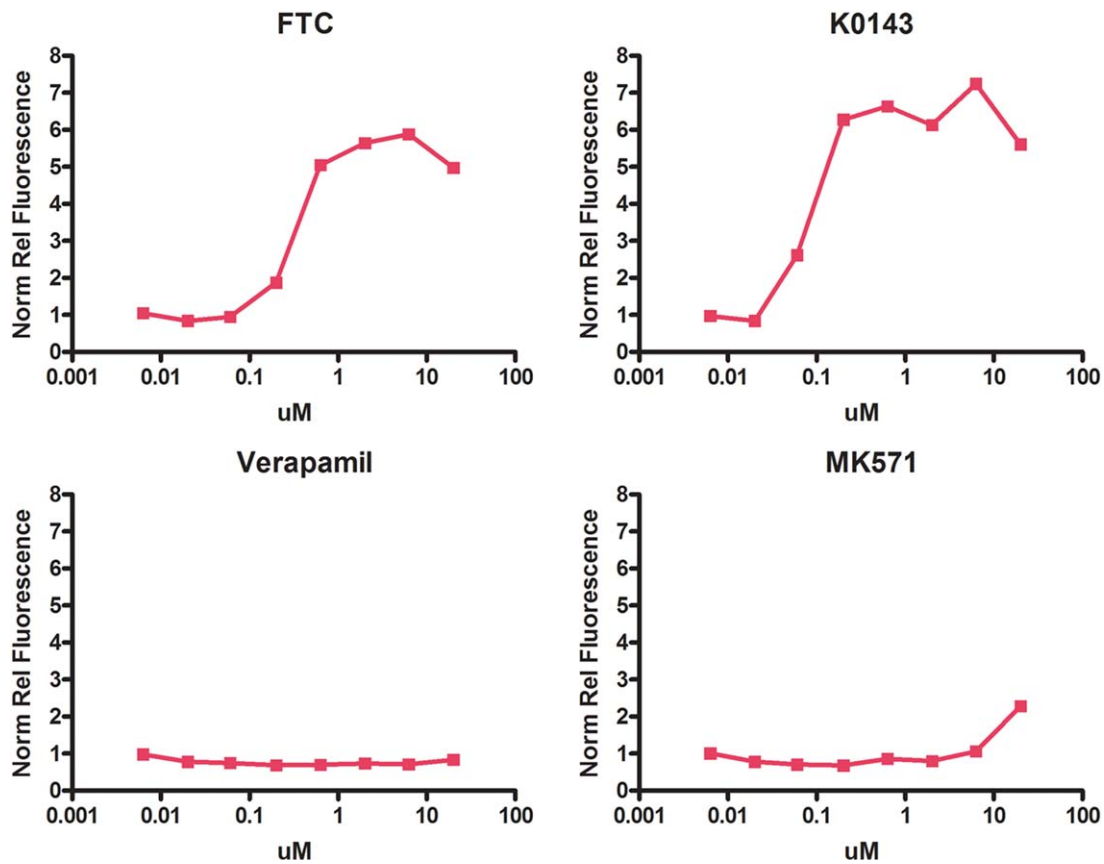fects were observed for either verapamil (ABCB1 inhibition) or MK571 (ABCC1 inhibition). Treatment with chemical inhibitors was initiated on culture day 1. PhA (1 μM) was added 20 hr before culture termination on day 4. Relative fluorescence was normalized to cell number as determined by staining with RedDot1. Data are based upon a single experiment consisting of an average of culture plate well technical replicates.*

2012) were found to increase in expression. Up-regulation of TTr and Gata4 were observed as well.

Ttr a common marker of visceral endoderm and is expressed in definitive endoderm (Goh et al., 2014), it is also up-regulated in human cardiomyocytes (Synnergren et al., 2008). Gata4, is expressed in definitive endoderm (Rojas et al., 2010) but is also necessary for cardiomyocyte fate determination (Holtzinger et al., 2010) and is found in the murine heart (Arceci et al., 1993). Expression of the neuroectoderm markers, Nes (Lendahl et al., 1990) and Ncam1 (Bally-Cuif et al., 1993), did not change notably suggesting that the formation of ectodermal cell types was not favored under our culture conditions and is consistent with the observation that cardiomyocyte formation was the preferred lineage pathway. Transcripts for the three ABC drug resistance transporters were readily detectable and remained relatively uniform across the culture period (Fig. 1B).

K0143 INHIBITED ABCG2 ACTIVITY IN MESC

Maximum inhibition of ABCG2 was achieved using approximately 1 μM K0143 or FTC. Low PhA fluorescence was observed following treatment with either verapamil or MK571, thus confirming the specificity of PhA as a substrate for ABCG2 in mESC (Fig. 2).

ABCG2 IS AN EFFECTIVE XENOBIOTIC EFFLUX TRANSPORTER IN MESC

An established role for ABCG2 is to serve as an efflux transporter in a variety of tissues and cell types. This function was evaluated in mESC by exposing J1 cells on culture day 1 to K0143 in combination with chemotherapeutics known to be substrates of ABCG2. Effects on proliferation and differentiation were then evaluated on culture day 4. Inhibition of ABCG2 increased the toxicity associated with topotecan and mitoxantrone but, surprisingly, not doxorubicin where it is possible that transporter redundancy may have played a role (Fig. 3). Numerical fold change data and
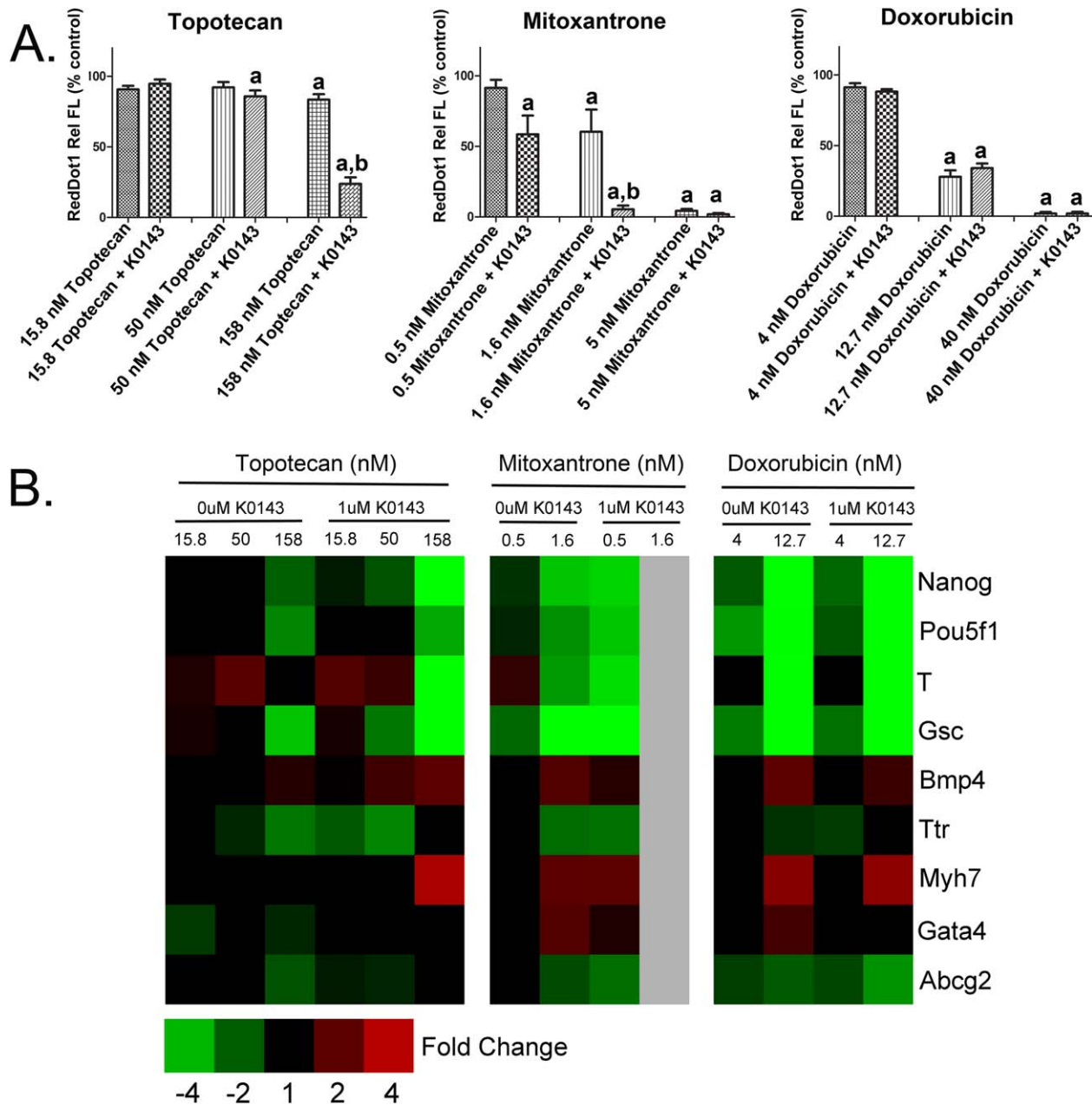
FIGURE 3. *ABCG2 and xenobiotic transport in mESC. Cell number (**A**) and gene expression (**B**) were evaluated on culture day 4 following initiation of treatment on culture day 1. Differential toxicity of topotecan and mitoxantrone, two chemotherapeutic agents, was observed following co-treatment with K0143. These data indicate that ABCG2 provides protection from certain xenobiotics during early development. a, significance from control ($p \leq 0.05$), b, significance from similarly treated group not exposed to K0143 ($p \leq 0.05$). Error bars, standard deviation.*

statistical significance for individual genes are provided in Supplementary Table S1, which is available online.

ABCG2 ACTIVITY INCREASES IN DIFFERENTIATING MESC

A significant increase in ABCG2 activity was observed when transporter function on culture day 1 was contrasted to that on culture day 4 (Fig. 4A). In this experiment, mESC were

co-treated with K0143 and PhA approximately 20 hr before evaluation of PhA fluorescence. These results were further supported using capillary-based immunoassay where a notable reduction in protein expression of ABCG2 was found on culture day 2, although the level of ABCG2 protein expression on culture day 0 was found to be similar to that observed on culture days 4 through 9 (Fig. 4B).
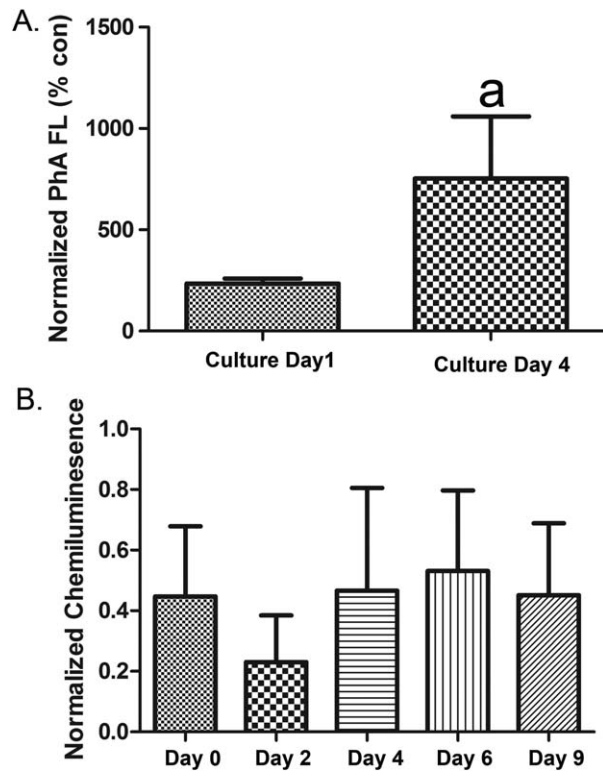
FIGURE 4. *ABCG2 activity in mESC. ABCG2 activity increased during early mESC differentiation based on retention of PhA. mESC were co-treated with K0143 (1 μM) and PhA (1 μM) approximately 20 hr before evaluation of fluorescence by plate scanning. Relative fluorescence was normalized to cell number as determined by staining with RedDot1 (**A**). Reduced expression of ABCG2 protein was observed on culture day 2 by capillary-based immunoassay. Note, similar results were obtained across two independent experiments with measured variation principally related to differences in relative signal between experiments (**B**). a, significance from control (p ≤ 0.05). Error bars = standard deviation.*

INHIBITION OF ABCG2 DOES NOT ALTER STEM CELL DIFFERENTIATION

Susanto et al. (2008) indicated that chemical or RNAi inhibition of ABCG2 in pluripotent mESC could alter the course of stem cell differentiation. To evaluate whether ABCG2 serves a fundamental role during early mESC differentiation, pluripotent mESC were seeded with and without K0143 on culture day 0 and cells were evaluated for changes in proliferation and differentiation on culture day 4. Cell number and gene expression were unchanged (Fig. 5).

ABCG2 INHIBITION DOES NOT ALTER THE TOXICITY OF TOXCAST PHASE I CHEMICALS

The effect of chemicals predicted by the ToxCast screening program to regulate ABCG2 was evaluated with and without co-treatment with K0143. As in our previous studies, exposures were initiated on culture day 1 and treatment effects evaluated on culture day 9 (Barrier et al., 2011; Chandler et al., 2011). Based on cell number and marker

gene expression, co-treatment with K0143 did not alter the toxicity induced by this group of xenobiotics (Fig. 6). While greater expression of Ttr was observed at the highest concentration of propiconazole, the change was not statistically significant. Numerical fold change data and statistical significance for individual genes are provided in Supplementary Table S2.

INHIBITION OF ABCG2 DOES NOT ALTER THE TOXICITY OF OXIDATIVE STRESSORS

Chandler et al. (2011) proposed altered redox homeostasis as a potential mode of action for ABCG2 and other pathways found to modify mESC differentiation. To evaluate the role of ABCG2 during redox challenge, mESC were treated with K0143 on culture day 3 along with known oxidative stressors and evaluated approximately 20 hr later. Negative effects on cell proliferation and gene expression were readily observable with either tert-Butyl hydroperoxide or paraquat; however, co-treatment with K0143 had no influence on the cytotoxicity induced by either treatment (Fig. 7). Numerical fold change data and statistical significance for individual genes are provided in Supplementary Table S3.

Discussion

The role of ABCG2 during mESC differentiation was evaluated with and without xenobiotic challenge. As a cell
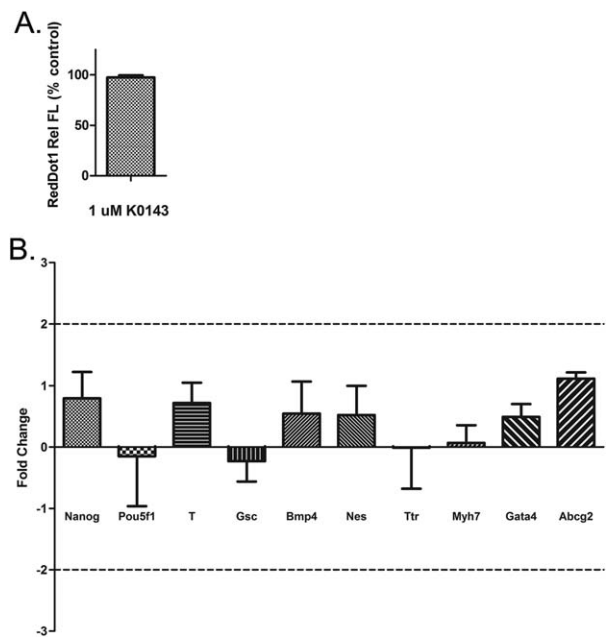

FIGURE 5. *Inhibition of ABCG2 and early mESC differentiation. Cell number (**A**) and gene expression (**B**) were evaluated on culture day 4 following initiation of treatment with K0143 on culture day 0. Inhibition of ABCG2 had no effect on cell proliferation or marker gene expression. Error bars, standard deviation.*

FIGURE 6. *ABCG2 inhibition and toxicity of EPA ToxCast chemicals. Cell number (***A***) and gene expression (***B***) in mESC exposed to propiconazole, flusilazole, pyridaben, rotenone, or imazapyr with or without co-treatment with 1 μM K0143. Cells were treated from culture day 1 through day 9. An interaction between chemical exposure and K0143 treatment was not observed as would be expected based on the hypothesis that certain xenobiotics influence mESC differentiation by altering ABCG2 activity. Imazapyr was included as a negative control. Error bars. standard deviation.*
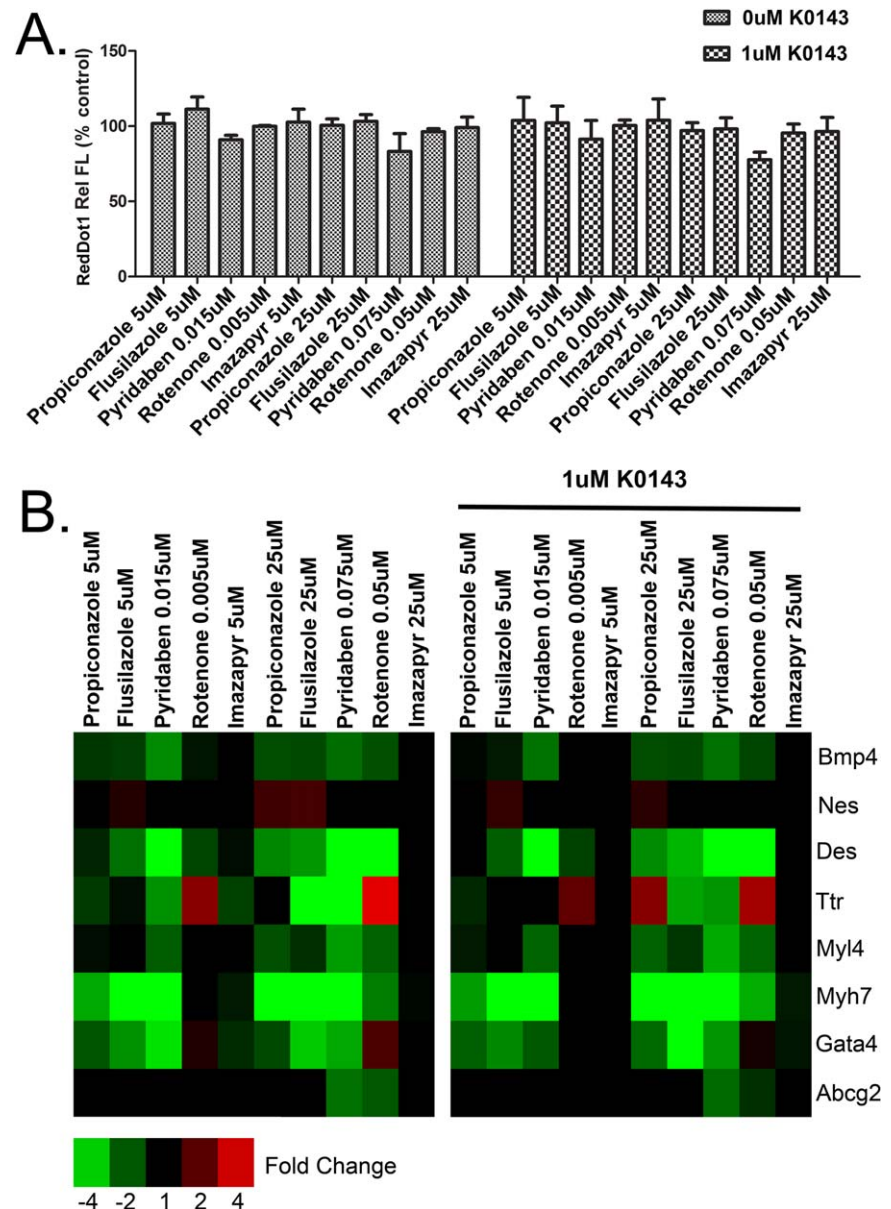
population average, the activity of ABCG2 was found to increase during early mESC differentiation. Although the established role of ABCG2 as a xenobiotic transporter could be demonstrated using known chemotherapeutic substrates, pharmacological inhibition of ABCG2 did not alter mESC differentiation suggesting that, at least when evaluated in an adherent culture system, ABCG2 is not essential to the early stages of mESC differentiation. In addition, inhibition of ABCG2 did not alter the toxicity of various ToxCast chemicals indicating that the transporter may not play a role in the mode of action of these chemicals, a hypothesis previously suggested by our group based on altered redox status. Along those lines, inhibition

of ABCG2 did not shift the toxicity of two oxidative stressors raising a question about the role of ABCG2 in regulating redox status during early mESC differentiation.

The adherent culture system used in this study was developed by our group as an alternative to assays which rely on hanging drop culture and embryoid body formation (Barrier et al., 2011). In this system, mESC are grown in two-dimensional (2D) adherent culture under maintenance growth conditions containing FBS. Once feeder cells and LIF are removed, there is a tendency for mESC to follow a differentiation path toward cardiomyocyte formation (Aouadi et al., 2006), although it should be stressed that mESC do not proliferate in culture as a synchronized
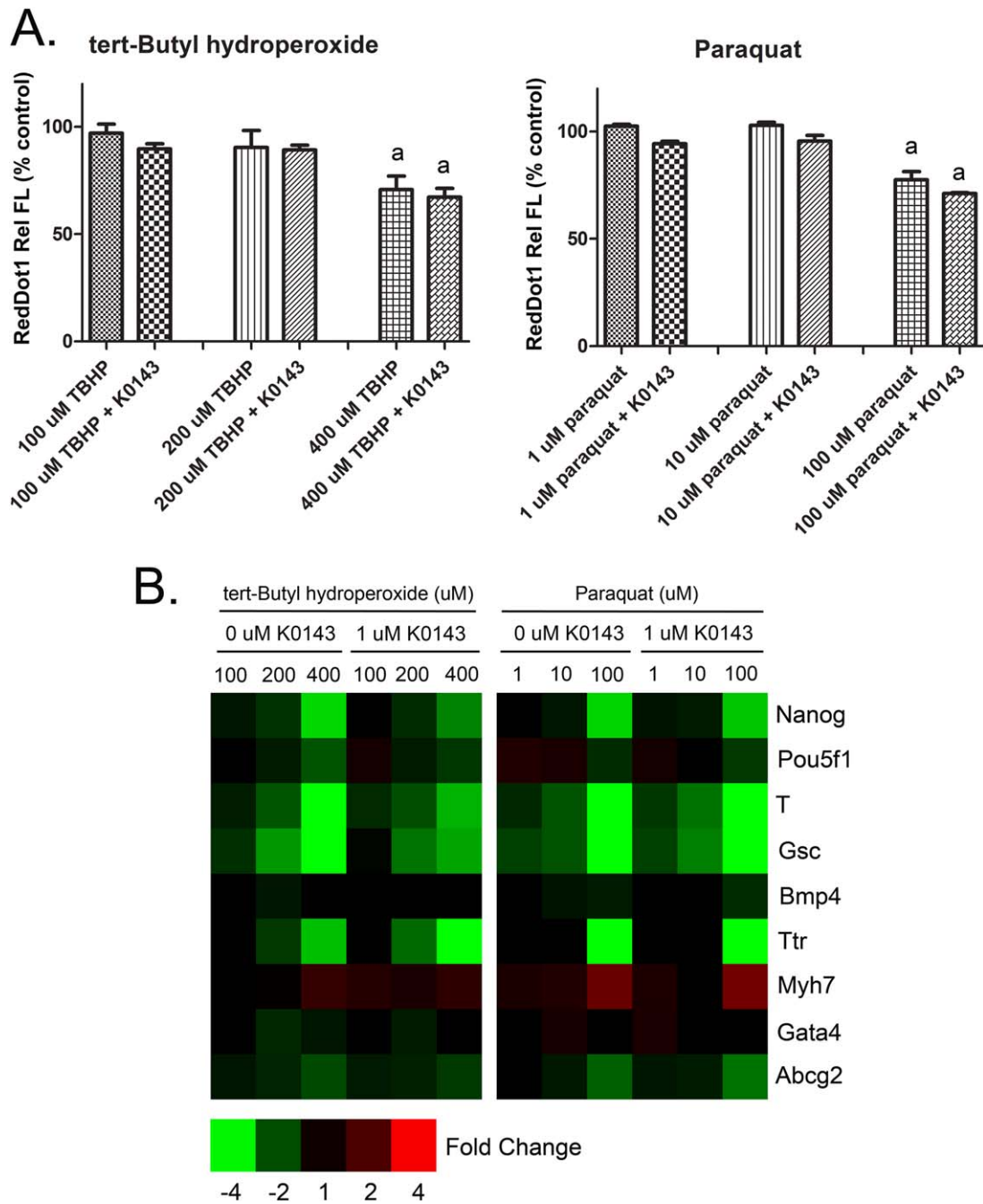
FIGURE 7. *ABCG2 and oxidative stress in mESC. Cell number (**A**) and gene expression (**B**) were evaluated on culture day 4 following initiation of treatment on culture day 3. Co-treatment with 1 μM K0143 did not shift the toxicity of either tert-Butyl hydroperoxide or paraquat thus raising a question about the role of ABCG2 in maintaining redox homeostasis during early mESC differentiation. a, significance from control (p ≤ 0.05). Error bars, standard deviation.*

population of cells, hence, it is likely that cells at different stages of differentiation and representing different lineages were present in our cultures. Based on changes in gene expression, this culture system provided a straightforward and dynamic system by which to evaluate mESC differentiation.

While increased ABCG2 activity might be an important characteristic of stem cell plasticity, or SP phenotype, in several tissues (Summer et al., 2003; Martin et al., 2004; Meeson et al., 2004; Cervello et al., 2010; Oka et al., 2010; Fatima et al., 2012; Foster et al., 2013) it is not clear that is the case in embryonic stem cells. Apati et al. (2008)

reported that both mRNA and protein levels of ABCG2 drop significantly in human embryonic stem cells (hESC) following differentiation, however, conflicting data were reported by Zeng et al. (2009). This was clarified by Padmanabhan et al. (2012), who found moderate levels of ABCG2 transcript but no measurable protein in nondifferentiated hESC cells. Erdei et al. (2013) further reported that ABCG2 expression was not uniformly observed in pluripotent hESC. The relationship between ABCG2 and embryonic stem cell plasticity in mouse cells is also uncertain. Sawicki et al. (2006) observed Abcg2 expression in both the murine blastula as well as early stage embryos, and Zeng et al. (2009) found ABCG2 protein in both undifferentiated and differentiated mESC.

Vieyra et al. (2009), on the other hand, identified a distinct but somewhat heterogenous population of pluripotent mESC that exhibited low Hoechst fluorescence along with somewhat higher levels of Abcg2, Abcb1, and Abcc3 transcript, although the role of ABCG2 was not specifically addressed. The question as to whether a subset of SP cells can be found within the larger population of mESC was not the focus of the current study; however, pluripotent mESC were exposed to K0143, a specific inhibitor of ABCG2, without negative effects on proliferation or early differentiation. Thus, at least at the level of inhibition typically achieved by pharmacological compounds, reduced activity of ABCG2 was not sufficient to disrupt normal differentiation when pluripotent mESC were evaluated in an adherent cell culture system. This supports the contention that ABCG2 may not play a fundamental role in early differentiation and is consistent with the observation that ABCG2-null mice develop normally (Jonker et al., 2002).

An increase in ABCG2 transporter activity along with a corresponding increase in ABCG2 protein expression was also observed as mESC transitioned to a differentiated state, although a relatively high level of ABCG2 protein on culture day 0 was noted in our study as well. Whether a decrease in ABCG2 activity after initial seeding of cells is a true reflection of the biology of mESC or might somehow be related to how these cells behave under in vitro conditions is not clear. As cells of the inner cell mass, J1 embryonic stem cells represent cells of the hypoblast and amniotic ectoderm as well as those of the embryonic epiblast. How these extraembryonic cells proliferate after initial plating is not certain but shifting cell populations during the first few days of cell culture could contribute to our results. Nevertheless, these data provide general support to observations previously made in hESC which suggest that ABCG2 activity increases during the early stages of stem cell differentiation, at least within certain cell lineages (Padmanabhan et al., 2012).

An important finding of this study was that ABCG2 is not associated with the toxicity of ToxCast Phase I compounds in mESC as previously theorized by our group (Chandler et al., 2011). Twenty-two chemicals were

originally observed to be positive in both our in-house stem cell assay as described by Barrier et al. (2011) as well as the phase I ToxCast transcription activation assay for ABCG2 which used primary human hepatocytes. This group of chemicals drove the statistical significance discussed by Chandler et al. (2011). Only nine of these chemicals were found to alter stem cell differentiation, with the remaining compounds causing cytotoxicity. Four of the nine chemicals were then evaluated in the current study with no interaction being observed between chemical inhibition of ABCG2 and xenobiotic induced effects. While this study was not broad in nature, we nevertheless believe it unlikely that ABCG2 activity is related to the toxicity previously observed by our group.

A more credible explanation lies in the complex regulation of ABCG2 (reviewed by Nakanishi and Ross, 2012). The cis-regulatory elements within the ABCG2 promoter include HRE (Krishnamurthy et al., 2004) and ARE (Singh et al., 2010), potentially linking ABCG2 activity to the cellular response to hypoxia and oxidative stress. Furthermore, regulation of ABCG2 by PXR has been demonstrated in human cells (Lemmen et al., 2013) as has regulation by AhR (Tan et al., 2010; To et al., 2011), although comparable regulation of ABCG2 by AhR is less clear in mouse cells (Tan et al., 2010). ABCG2 has also been shown to be regulated by both PPARα (Eldasher et al., 2013) and PPARγ (Szatmari et al., 2006) which links ABCG2 activity to compounds that act as peroxisome proliferators. Hence, it is likely that regulation of ABCG2 is associated with xenobiotic exposure in certain cells types. Several of these xenobiotics would also be expected to show biological activity in mESC; however, this relationship would not necessarily be one of cause and effect. It is also worth noting that up-regulation of Abcg2 transcript was not observed in these experiments. Hence, regulation of Abcg2 in mESC may differ from that observed in primary human hepatocytes, the cell type used in the ToxCast ABCG2 transcription activation assay.

The idea that ABCG2 may play a role in regulating redox status in mESC is well supported in the literature. Transcriptional regulation of Abcg2 is influenced by HIF-1, and ABCG2 has been shown to provide protection from hypoxic condition in murine hematopoietic stem cells by transporting excess porphyrins (Krishnamurthy et al., 2004). Indeed, transport of porphyrins such as protoporphyrin IX, heme, and hemin is an established function of ABCG2 (Jonker et al., 2002; Robey et al., 2005; Zhou et al., 2005; Desuzinges-Mandon et al., 2010), and mitochondrial damage associated with elevated levels of protoporphyrin IX has been observed in hepatocytes from Abcg2-null mice (Lin et al., 2013). ABCG2 has also been shown to be regulated by NRF2 (NFE2L2) in human cells (Adachi et al., 2007; Singh et al., 2010) and in rodents (Wang et al., 2014).

Transport of glutathione may be yet a third mechanism by which ABCG2 could influence redox status in mESC (Brechbuhl et al., 2010; Higashikuni et al., 2012), although

conflicting data have been reported (Gauthier et al., 2013). Nevertheless, Zeng et al. (2012) found that reduced ABCG2 activity was associated with lower levels of gluta-thione and increased oxidative stress in the central nerv-ous system of a transgenic murine model for Alzheimer's disease, and Krzyzanowski et al. (2014) reported that overexpression of ABCG2 actually exacerbated the response to oxidative stress in HepG2 cells potentially due to increased efflux of glutathione. Hence, a link between ABCG2 function and redox homeostasis might be expected in mESC. It was, therefore, surprising that inhibition of ABCG2 in mESC had no effect on the toxicity induced by either tert-butyl hydroperoxide or paraquat and that tran-scriptional regulation of Abcg2 was unaffected by oxidative stress. These results require confirmation in other vitro models. It is possible that the effects of ABCG2 in the cur-rent study were not apparent as a cell population average or that additional experimental times points were needed to observe an effect. It is also possible that the treatments used were in excess of the capacity for ABCG2 to modulate redox status or that mESC grown in 2D culture may not adequately reflect the in vivo environment of the early embryo with regard to redox homeostasis.

In summary, the role of ABCG2 during the early stages of mESC differentiation was examined both with and with-out xenobiotic challenge using pharmacological inhibition of ABCG2. Reduced ABCG2 activity did not alter normal early mESC differentiation and did not shift the toxicity of compounds predicted by ToxCast to regulate ABCG2. An increase in transporter activity was observed during early lineage differentiation. The supposition that a mechanistic link exists between ABCG2 activity and xenobiotic toxicity was not supported, although, a protective role for ABCG2 as a xenobiotic transporter was reaffirmed in mESC as it has in other cells. Inhibition of ABCG2 did not shift the toxicity of tert-Butyl hydroperoxide or paraquat thus rais-ing a question about the role of ABCG2 in maintaining redox homeostasis during early mESC differentiation. As we continue to develop predictive models for developmen-tal toxicants, modulation of ABCG2 activity may serve as a useful endpoint. The current study, however, argues against altered ABCG2 activity as a critical molecular ini-tiating event associated with xenobiotic-induced dysmor-phology during early development.

Acknowledgments

References

Adachi T, Nakagawa H, Chung I, et al. 2007. Nrf2-dependent and -independent induction of ABC transporters ABCC1, ABCC2, and ABCG2 in HepG2 cells under oxidative stress. J Exp Ther Oncol 6:335–348.

Allen JD, van Loevezijn A, Lakhai JM, et al. 2002. Potent and spe-cific inhibition of the breast cancer resistance protein multidrug transporter in vitro and in mouse intestine by a novel analogue of fumitremorgin C. Mol Cancer Ther 1:417–425.

Aouadi M, Bost F, Caron L, et al. 2006. p38 mitogen-activated protein kinase activity commits embryonic stem cells to either neurogenesis or cardiomyogenesis. Stem Cells 24:1399–1406.

Apati A, Orban TI, Varga N, et al. 2008. High level functional expression of the ABCG2 multidrug transporter in undifferenti-ated human embryonic stem cells. Biochim Biophys Acta 1778: 2700–2709.

Arceci RJ, King AA, Simon MC, et al. 1993. Mouse GATA-4: a reti-noic acid-inducible GATA-binding transcription factor expressed in endodermally derived tissues and heart. Mol Cell Biol 13: 2235–2246.

Bag S, Pfannkuche K, Krzyzak V, et al. 2012. Derivation of es cells from early stage preimplantation embryos and characterisation of their cardiac differentiation potential in mice. J Stem Cells Regen Med 8:12–20.

Bally-Cuif L, Goridis C, Santoni MJ. 1993. The mouse NCAM gene displays a biphasic expression pattern during neural tube devel-opment. Development 117:543–552.

Barrier M, Jeffay S, Nichols HP, et al. 2011. Mouse embryonic stem cell adherent cell differentiation and cytotoxicity (ACDC) assay. Reprod Toxicol 31:383–391.

Brechbuhl HM, Gould N, Kachadourian R, et al. 2010. Glutathione transport is a unique function of the ATP-binding cassette pro-tein ABCG2. J Biol Chem 285:16582–16587.

Bunting KD. 2002. ABC transporters as phenotypic markers and functional regulators of stem cells. Stem Cells 20:11–20.

Cervello I, Gil-Sanchis C, Mas A, et al. 2010. Human endometrial side population cells exhibit genotypic, phenotypic and func-tional features of somatic stem cells. PLoS One 5:e10964.

Chandler KJ, Barrier M, Jeffay S, et al. 2011. Evaluation of 309 environmental chemicals using a mouse embryonic stem cell adherent cell differentiation and cytotoxicity assay. PLoS One 6: e18540.

Christoforou N, Miller RA, Hill CM, et al. 2008. Mouse ES cell-derived cardiac precursor cells are multipotent and facilitate identification of novel cardiac genes. J Clin Invest 118:894–903.

De Robertis EM, Fainsod A, Gont LK, Steinbeisser H. 1994. The evolution of vertebrate gastrulation. Dev Suppl :117–124.

Desuzinges-Mandon E, Arnaud O, Martinez L, et al. 2010. ABCG2 transports and transfers heme to albumin through its large extracellular loop. J Biol Chem 285:33123–33133.

Ding XW, Wu JH, Jiang CP. 2010. ABCG2: a potential marker of stem cells and novel target in stem cell and cancer therapy. Life Sci 86(17-18):631–637.

Eldasher LM, Wen X, Little MS, et al. 2013. Hepatic and renal Bcrp transporter expression in mice treated with perfluorooctanoic acid. Toxicology 306:108–113.

Erdei Z, Sarkadi B, Brozik A, et al. 2013. Dynamic ABCG2 expression in human embryonic stem cells provides the basis for stress response. Eur Biophys J 42(2-3):169–179.

Fatima S, Zhou S, Sorrentino BP. 2012. Abcg2 expression marks tissue-specific stem cells in multiple organs in a mouse progeny tracking model. Stem Cells 30:210–221.

Foster BA, Gangavarapu KJ, Mathew G, et al. 2013. Human prostate side population cells demonstrate stem cell properties in recombination with urogenital sinus mesenchyme. PLoS One 8:e55062.

Gauthier C, Ozvegy-Laczka C, Szakacs G, et al. 2013. ABCG2 is not able to catalyze glutathione efflux and does not contribute to GSH-dependent collateral sensitivity. Front Pharmacol 4:138.

Goh HN, Rathjen PD, Familari M, Rathjen J. 2014. Endoderm complexity in the mouse gastrula is revealed through the expression of spink3. Biores Open Access 3:98–109.

Goodell MA, Brose K, Paradis G, et al. 1996. Isolation and functional properties of murine hematopoietic stem cells that are replicating in vivo. J Exp Med 183:1797–1806.

Hardwick LJ, Velamakanni S, van Veen HW. 2007. The emerging pharmacotherapeutic significance of the breast cancer resistance protein (ABCG2). Br J Pharmacol 151:163–174.

Henrich CJ, Bokesch HR, Dean M, et al. 2006. A high-throughput cell-based assay for inhibitors of ABCG2 activity. J Biomol Screen 11:176–183.

Higashikuni Y, Sainz J, Nakamura K, et al. 2012. The ATP-binding cassette transporter ABCG2 protects against pressure overload-induced cardiac hypertrophy and heart failure by promoting angiogenesis and antioxidant response. Arterioscler Thromb Vasc Biol 32:654–661.

Hofner M, Hollrigl A, Puz S, et al. 2007. Desmin stimulates differentiation of cardiomyocytes and up-regulation of brachyury and nkx2.5. Differentiation 75:605–615.

Holtzinger A, Rosenfeld GE, Evans T. 2010. Gata4 directs development of cardiac-inducing endoderm from ES cells. Dev Biol 337:63–73.

Jonker JW, Buitelaar M, Wagenaar E, et al. 2002. The breast cancer resistance protein protects against a major chlorophyll-derived dietary phototoxin and protoporphyria. Proc Natl Acad Sci U S A 99:15649–15654.

Kattman SJ, Witty AD, Gagliardi M, et al. 2011. Stage-specific optimization of activin/nodal and BMP signaling promotes cardiac differentiation of mouse and human pluripotent stem cell lines. Cell Stem Cell 8:228–240.

Kim M, Morshead CM. 2003. Distinct populations of forebrain neural stem and progenitor cells can be isolated using side-population analysis. J Neurosci 23:10703–10709.

Krishnamurthy P, Ross DD, Nakanishi T, et al. 2004. The stem cell marker Bcrp/ABCG2 enhances hypoxic cell survival through interactions with heme. J Biol Chem 279:24218–24225.

Krzyzanowski D, Bartosz G, Grzelak A. 2014. Collateral sensitivity: ABCG2-overexpressing cells are more vulnerable to oxidative stress. Free Radic Biol Med 76:47–52.

Lemmen J, Tozakidis IE, Galla HJ. 2013. Pregnane X receptor upregulates ABC-transporter Abcg2 and Abcb1 at the blood-brain barrier. Brain Res 1491:1–13.

Lendahl U, Zimmerman LB, McKay RD. 1990. CNS stem cells express a new class of intermediate filament protein. Cell 60:585–595.

Lin YH, Chang HM, Chang FP, et al. 2013. Protoporphyrin IX accumulation disrupts mitochondrial dynamics and function in ABCG2-deficient hepatocytes. FEBS Lett 587:3202–3209.

Livak KJ, Schmittgen TD. 2001. Analysis of relative gene expression data using real-time quantitative PCR and the 2(-Delta Delta C(T)) Method. Methods 25:402–408.

Martin CM, Meeson AP, Robertson SM, et al. 2004. Persistent expression of the ATP-binding cassette transporter, Abcg2, identifies cardiac SP cells in the developing and adult heart. Dev Biol 265:262–275.

Meeson AP, Hawke TJ, Graham S, et al. 2004. Cellular and molecular regulation of skeletal muscle side population cells. Stem Cells 22:1305–1320.

Mitsui K, Tokuzawa Y, Itoh H, et al. 2003. The homeoprotein Nanog is required for maintenance of pluripotency in mouse epiblast and ES cells. Cell 113:631–642.

Mo W, Zhang JT. 2012. Human ABCG2: structure, function, and its role in multidrug resistance. Int J Biochem Mol Biol 3:1–27.

Nakanishi T, Ross DD. 2012. Breast cancer resistance protein (BCRP/ABCG2): its role in multidrug resistance and regulation of its gene expression. Chin J Cancer 31:73–99.

Nichols J, Zevnik B, Anastassiadis K, et al. 1998. Formation of pluripotent stem cells in the mammalian embryo depends on the POU transcription factor Oct4. Cell 95:379–391.

Oka M, Toyoda C, Kaneko Y, et al. 2010. Characterization and localization of side population cells in the lens. Mol Vis 16:945–953.

Padmanabhan R, Chen KG, Gillet JP, et al. 2012. Regulation and expression of the ATP-binding cassette transporter ABCG2 in human embryonic stem cells. Stem Cells 30:2175–2187.

Robey RW, Steadman K, Polgar O, Bates SE. 2005. ABCG2-mediated transport of photosensitizers: potential impact on photodynamic therapy. Cancer Biol Ther 4:187–194.

Robey RW, To KK, Polgar O, et al. 2009. ABCG2: a perspective. Adv Drug Deliv Rev 61:3–13.

Rojas A, Schachterle W, Xu SM, et al. 2010. Direct transcriptional regulation of Gata4 during early endoderm specification is

controlled by FoxA2 binding to an intronic enhancer. Dev Biol 346:346–355.

Sarkadi B, Ozvegy-Laczka C, Nemet K, Varadi A. 2004. ABCG2 -- a transporter for all seasons. FEBS Lett 567:116–120.

Sawicki WT, Kujawa M, Jankowska-Steifer E, et al. 2006. Temporal/spatial expression and efflux activity of ABC transporter, P-glycoprotein/Abcb1 isoforms and Bcrp/Abcg2 during early murine development. Gene Expr Patterns 6:738–746.

Scharenberg CW, Harkey MA, Torok-Storb B. 2002. The ABCG2 transporter is an efficient Hoechst 33342 efflux pump and is preferentially expressed by immature human hematopoietic progenitors. Blood 99:507–512.

Sharom FJ. 2008. ABC multidrug transporters: structure, function and role in chemoresistance. Pharmacogenomics 9:105–127.

Singh A, Wu H, Zhang P, et al. 2010. Expression of ABCG2 (BCRP) is regulated by Nrf2 in cancer cells that confers side population and chemoresistance phenotype. Mol Cancer Ther 9:2365–2376.

Stacy AE, Jansson PJ, Richardson DR. 2013. Molecular pharmacology of ABCG2 and its role in chemoresistance. Mol Pharmacol 84:655–669.

Summer R, Kotton DN, Sun X, et al. 2003. Side population cells and Bcrp1 expression in lung. Am J Physiol Lung Cell Mol Physiol 285:L97–L104.

Susanto J, Lin YH, Chen YN, et al. 2008. Porphyrin homeostasis maintained by ABCG2 regulates self-renewal of embryonic stem cells. PLoS One 3:e4023.

Synnergren J, Akesson K, Dahlenborg K, et al. 2008. Molecular signature of cardiomyocyte clusters derived from human embryonic stem cells. Stem Cells 26:1831–1840.

Szatmari I, Vamosi G, Brazda P, et al. 2006. Peroxisome proliferator-activated receptor gamma-regulated ABCG2 expression confers cytoprotection to human dendritic cells. J Biol Chem 281:23812–23823.

Tan KP, Wang B, Yang M, et al. 2010. Aryl hydrocarbon receptor is a transcriptional activator of the human breast cancer resistance protein (BCRP/ABCG2). Mol Pharmacol 78:175–185.

To KK, Robey R, Zhan Z, et al. 2011. Upregulation of ABCG2 by romidepsin via the aryl hydrocarbon receptor pathway. Mol Cancer Res 9:516–527.

Vieyra DS, Rosen A, Goodell MA. 2009. Identification and characterization of side population cells in embryonic stem cell cultures. Stem Cells Dev 18:1155–1166.

Wang X, Campos CR, Peart JC, et al. 2014. Nrf2 upregulates ATP binding cassette transporter expression and activity at the blood-brain and blood-spinal cord barriers. J Neurosci 34:8585–8593.

Winnier G, Blessing M, Labosky PA, Hogan BL. 1995. Bone morphogenetic protein-4 is required for mesoderm formation and patterning in the mouse. Genes Dev 9:2105–2116.

Zeng H, Park JW, Guo M, et al. 2009. Lack of ABCG2 expression and side population properties in human pluripotent stem cells. Stem Cells 27:2435–2445.

Zeng Y, Callaghan D, Xiong H, et al. 2012. Abcg2 deficiency augments oxidative stress and cognitive deficits in Tg-SwDI transgenic mice. J Neurochem 122:456–469.

Zhou S, Schuetz JD, Bunting KD, et al. 2001. The ABC transporter Bcrp1/ABCG2 is expressed in a wide variety of stem cells and is a molecular determinant of the side-population phenotype. Nat Med 7:1028–1034.

Zhou S, Zong Y, Ney PA, et al. 2005. Increased expression of the Abcg2 transporter during erythroid maturation plays a role in decreasing cellular protoporphyrin IX levels. Blood 105:2571–2576.

Supplementary Table 1. Average Fold Change on Culture Day 4 in mESC exposed to chemotherapeutics with and without K0143 co-treatment[1].

Trt	K0143	T	Gsc	Pou5fl	Nanog	Ttr	Bmp4	Gata4	Myh7	Abcg2
Topotecan 15.8nM	0 µM	1.35±0.22	1.29±0.08	-0.37±1.82	-0.37±1.26	0.66±1.49	-0.39±1.24	-1.52±0.37	-0.49±1.33	-0.41±1.33
Topotecan 50nM	0 µM	1.91±0.86	-1.12±0.12	0.26±1.53	-0.50±1.33	-1.39±2.17	1.11±0.09	-0.82±1.59	-0.58±1.46	0.43±1.59
Topotecan 158nM	0 µM	0.37±1.29	-4.46±0.83*	-2.76±2.00	-2.02±0.34*	-2.43±0.57	1.37±0.18	-1.39±0.09	-0.37±1.33	-1.84±0.39*
Mitoxantrone 0.5nM	0 µM	1.48±0.44	-2.17±0.13*	-1.37±0.34	-1.48±0.11	-0.31±2.19	1.14±0.04	0.58±1.47	0.34±1.36	-0.46±1.36
Mitoxantrone 1.6nM	0 µM	-3.30±1.19*	-14.02±2.66*	-2.98±1.15	-4.46±1.65*	-2.24±0.22	1.81±0.23*	1.78±0.52	1.94±0.23*	-1.71±0.13
Doxorubicin 4nM	0 µM	-0.19±1.58	-2.57±0.29*	-3.20±1.59	-1.93±0.05*	-0.58±1.71	1.13±0.04	-0.24±1.71	-0.34±1.46	-1.58±0.35
Doxorubicin 12.7nM	0 µM	-12.96±3.38*	-20.91±0.59*	-6.40±3.19*	-9.68±2.56*	-1.48±2.56	1.96±0.23*	1.61±0.73	2.74±0.24*	-1.94±0.28*
Topotecan 15.8nM	1 µM	1.79±0.29	1.28±0.03	0.29±1.83	-1.31±0.11	-1.92±2.86	1.17±0.12	-0.49±1.41	-0.37±1.27	-1.30±0.23
Topotecan 50nM	1 µM	1.53±0.42	-2.45±0.65*	-0.61±1.57	-1.83±0.26	-2.78±2.69	1.60±0.20*	0.46±1.35	0.69±1.57	-1.36±0.25
Topotecan 158nM	1 µM	-17.23±5.05*	-9.54±4.00*	-3.59±0.53	-8.53±1.38*	-0.86±2.31	1.95±0.72*	0.61±1.55	3.66±1.89*	-0.75±1.59
Mitoxantrone 0.5nM	1 µM	-5.21±3.32*	-13.87±3.56*	-4.48±3.53	-4.92±2.05*	-2.36±1.15	1.39±0.15*	1.33±0.15	1.99±0.43*	-2.29±0.74
Mitoxantrone 1.6nM	1 µM	no RNA	no RNA	no RNA	no RNA	no RNA	no RNA	no RNA	no RNA	no RNA
Doxorubicin 4nM	1 µM	0.40±1.50	-2.35±0.31*	-1.87±1.21	-2.16±0.42*	-1.57±0.36	0.42±1.28	0.21±1.75	0.34±1.17	-1.66±0.51
Doxorubicin 12.7nM	1 µM	-10.06±5.39*	-16.42±4.27*	-8.52±2.74*	-10.26±1.89*	-0.55±1.45	1.55±0.12*	-0.51±1.41	2.93±0.61*	-3.08±0.49*

[1]Values = mean±SD

* Significantly different than concurrent control ($p \leq 0.05$)

Supplementary Table 2. Average Fold Change on Culture Day 9 in xenobiotic-exposed mESC with and without K0143 co-treatment[1].

Trt	K0143	Bmp4	Nes	Des	Ttr	Myl4	Myh7	Gata4	Abcg2
Propiconazole 5 μM	0 μM	-1.60±0.37	-0.29±1.30	-1.48±0.27	-1.65±0.12	-1.33±0.14	-3.29±0.71	-1.94±0.37	-0.54±1.44
Flusilazole 5 μM	0 μM	-1.68±0.21	1.47±0.22	-2.34±0.32*	-1.33±2.54	-0.83±1.61	-10.50±1.00*	-2.85±0.58	-1.28±0.15
Pyridaben .015 μM	0 μM	-2.74±1.28*	-0.37±1.32	-11.18±7.53*	-2.85±5.19	-2.06±0.67*	-12.42±10.12*	-4.48±3.69*	-0.48±1.31
Rotenone 0.005 μM	0 μM	-1.38±0.23	-0.04±1.13	-1.76±0.27	2.71±0.60	-0.03±1.15	-1.03±0.93	1.46±0.16	0.00±1.33
Imazapyr 5 μM	0 μM	-1.21±0.04	-1.19±0.19	-1.33±0.22	-1.73±0.68	-1.13±0.07	-1.42±0.34	-1.54±0.33	-0.42±1.27
Propiconazole 25 μM	0 μM	-1.86±0.74	1.66±0.15	-2.70±0.93*	-0.12±6.08	-1.88±0.60	-10.54±0.82*	-1.81±0.55	0.33±1.30
Flusilazole 25 μM	0 μM	-1.80±0.68	1.74±0.28	-2.97±1.43*	-22.69±33.6	-1.57±0.46	-13.15±3.74*	-3.96±2.56*	-0.32±1.41
Pyridaben .075 μM	0 μM	-2.26±0.76*	-1.27±1.08	-19.55±7.08*	-7.75±7.68	-3.07±0.40*	-17.08±13.49*	-3.27±2.61	-2.34±0.46*
Rotenone 0.05 μM	0 μM	-1.90±0.31*	-0.05±1.11	-8.86±5.6*	4.53±3.13	-2.14±0.39*	-2.51±1.51	1.85±0.54	-1.98±0.57*
Imazapyr 25 μM	0 μM	-1.11±0.02	-0.22±1.53	-1.10±0.05	-0.96±2.02	-1.10±0.03	-1.32±0.03	-0.41±1.48	1.15±0.12
Propiconazole 5 μM	1 μM	-1.32±0.07	1.27±0.17	-1.23±0.05	-1.49±0.44	-1.42±0.44	-3.04±1.39	-2.07±0.67	0.33±1.30
Flusilazole 5 μM	1 μM	-1.42±0.16	1.59±0.10	-2.06±0.06	0.14±1.57	-0.75±1.78	-8.79±3.59*	-2.71±0.99	-1.25±0.18
Pyridaben .015 μM	1 μM	-2.37±1.05*	1.12±0.13	-10.47±5.93*	-0.50±2.75	-2.17±0.60*	-11.77±7.27*	-2.01±0.22	-0.39±1.46
Rotenone 0.005 μM	1 μM	-0.95±0.81	0.05±1.36	-1.71±0.49	2.07±2.89	-0.36±1.35	-0.59±1.51	1.21±0.94	0.07±1.17
Imazapyr 5 μM	1 μM	-1.10±0.05	-0.43±1.33	-0.36±21.22	-0.84±1.61	-0.39±1.22	-0.58±1.47	-1.19±0.04	0.38±1.22
Propiconazole 25 μM	1 μM	-1.87±0.74	1.52±0.33	-2.73±0.53*	2.69±1.72	-2.14±0.84*	-9.96±3.04*	-2.23±1.11	-1.09±0.09
Flusilazole 25 μM	1 μM	-1.82±0.59	0.81±1.63	-3.51±1.43*	-3.21±1.14	-1.62±0.56	-16.68±4.41*	-5.58±3.16*	-1.21±0.16
Pyridaben .075 μM	1 μM	-2.34±0.82*	-1.10±0.05	-20.71±6.46*	-2.94±5.88	-3.33±0.83*	-18.94±13.00*	-2.93±1.47	-2.22±0.11*
Rotenone 0.05 μM	1 μM	-1.75±0.56*	0.05±1.20	-7.77±4.49*	3.17±1.19	-2.15±0.31*	-3.34±3.07*	1.40±1.22	-1.56±0.39
Imazapyr 25 μM	1 μM	-1.14±0.10	0.25±1.45	-1.25±0.18	-0.72±1.51	-0.48±1.29	-1.43±0.29	-1.39±0.23	-1.12±0.06

[1]Values = Mean±SD

*Significantly different than concurrent control (p≤0.05)

Supplementary Table 3. Average Fold Change on Culture Day 4 in mESC exposed to oxidative stress with and without chemical inhibition of ABCG2[1]

Trt	K0143	T	Gsc	Pou5f1	Nanog	Ttr	Bmp4	Gata4	Myh7	Abcg2
TBHP 100 µM	0 µM	-1.27±0.17	-1.58±0.16	0.37±1.20	-1.12±0.13	-0.46±1.86	0.38±1.26	-0.41±1.43	0.52±1.47	-1.12±0.04
TBHP 200 µM	0 µM	-2.14±0.49	-2.95±0.76*	-1.22±0.18	-1.60±0.13*	-1.71±3.11	-1.13±0.10	-1.44±0.15	0.73±1.67	-1.37±0.12*
TBHP 400 µM	0 µM	-4.48±1.37*	-7.40±4.84*	-2.08±0.18*	-3.68±0.82*	-3.40±1.45	0.30±1.35	-1.12±0.07	1.64±0.24*	-1.95±0.13*
Paraquat 1 µM	0 µM	-1.44±0.07	-1.82±0.11	1.32±0.14	0.35±1.28	0.41±1.70	-0.33±1.18	0.44±1.30	1.21±0.06	0.30±1.26
Paraquat 10 µM	0 µM	-2.07±0.21*	-2.08±0.29*	1.20±0.11	-1.11±0.04	-0.28±2.57	-1.08±0.06	1.17±0.10	1.33±0.29	-1.16±0.02*
Paraquat 100 µM	0 µM	-8.89±4.28*	-7.71±4.06*	-1.51±0.18*	-3.64±1.36*	-4.75±1.83*	-1.22±0.08*	0.31±1.24	2.36±0.28*	-2.24±0.28*
TBHP 100 µM	1 µM	-1.47±0.13	-0.74±1.52	1.08±0.09	-0.45±1.26	-0.31±2.58	0.34±1.25	-0.49±1.63	1.37±0.33	-1.18±0.03
TBHP 200 µM	1 µM	-2.04±0.72	-2.50±0.37*	-1.22±0.25	-1.50±0.48	-2.38±0.99*	-0.40±1.33	-1.25±0.23	1.19±0.24	-1.34±0.15*
TBHP 400 µM	1 µM	-3.26±1.56*	-3.10±1.88*	-1.68±0.35*	-2.70±0.42*	-6.52±11.19	-0.36±1.24	-0.46±1.67	1.53±0.03*	-1.72±0.14*
Paraquat 1 µM	1 µM	-1.66±0.17	-1.82±0.31	1.07±0.08	-1.08±0.03	-0.22±1.70	-0.33±1.24	1.20±0.21	1.23±0.17	-1.14±0.08
Paraquat 10 µM	1 µM	-2.48±0.52*	-2.65±1.02*	0.39±1.22	-1.20±0.08	0.18±1.57	-0.45±1.26	0.35±1.32	-0.30±1.39	-1.25±0.16
Paraquat 100 µM	1 µM	-7.06±2.42*	-4.71±1.62*	-1.70±0.39*	-3.48±1.05*	-4.18±0.95*	-1.50±0.08*	0.41±1.35	2.47±0.59*	-2.47±0.53*

[1]Values = mean±SD

* Significantly different than concurrent control ($p \leq 0.05$)